

Ab initio g -tensor calculation for paramagnetic surface states: hydrogen adsorption at Si surfaces

U. Gerstmann^{*,1,2}, M. Rohrmüller¹, F. Mauri², and W.G. Schmidt¹

¹ Universität Paderborn, Lehrstuhl für Theoretische Physik, Warburger Str. 100, 33098 Paderborn, Germany

² Institut de Minéralogie et de Physique des Milieux Condensés, Université Pierre et Marie Curie, Campus Boucicaut, 140 rue de Lourmel, 75015 Paris, France

Received 5 July 2009, revised 30 October 2009, accepted 6 November 2009

Published online 25 January 2010

PACS 71.55.Cn, 71.70.Ej, 73.20.At, 73.20.Hb, 75.70.Rf

* Corresponding author: e-mail gerstmann@phys.upb.de, Phone: +49-5251-603481, Fax: +49-5251-603435

Ab initio calculations of the electronic g -tensor of paramagnetic states at surfaces are presented taking the adsorption of hydrogen atoms at silicon surfaces as an example. We show that for silicon surfaces with different hydrogen coverages, the g -tensor is by far more characteristic than the hyperfine splitting of the Si dangling bonds or the adsorbed H atoms.

This holds also in the case of powder spectra (e.g. amorphous or microcrystalline material) where only the angular average of the spectra is available from experiments. Hence, the *ab initio* calculation of the g -tensor should be in general a basic key to a better understanding of the microscopic structure of paramagnetic surfaces or interfaces.

© 2010 WILEY-VCH Verlag GmbH & Co. KGaA, Weinheim

1 Introduction Electron paramagnetic resonance (EPR) provides a powerful tool to analyse the microscopic structure of paramagnetic systems. In many cases, however, the wealth of important information available from EPR measurements, cannot be extracted from experimental data alone. For an identification of the microscopic structures, accurate first principles calculations of as many as possible relevant properties are necessary to calculate a fingerprint of the structure that can be compared with the experimental values. From EPR experiments the components of the electronic g -tensor are available also in those cases in which hyperfine (hf) splittings cannot be resolved. However, in contrast to the *ab initio* calculation of hf splittings that already do have an appreciable history, quantitative predictions of electronic g -tensors making use of the machinery of *ab initio* density functional theory (DFT) have become possible only very recently [1]. In semiconductors, this has been already demonstrated successfully for defects in SiC and GaN bulk material [2–4]. For surfaces, however, theoretical data obtained by *first principle* calculation was so far not available. Hydrogenated microcrystalline silicon ($\mu\text{c-Si:H}$) provides a very interesting example. The material can be used for efficient and low-cost solar cells [5],

that in comparison with cells based on amorphous silicon suffer less from the notorious light-induced degradation, known as the Staebler-Wronski effect [6]. Best cell performance is, however, achieved for material grown close to the transition to amorphous growth [7]. The porosity of this material allows in-diffusion of atmospheric gases [8]. The main effects to consider are, thus, adsorption and oxidation on surfaces. Oxidation would provide a non-reversible process with the occurrence of the fingerprint of the well-known P_b -centers (Si-O/Si interface dangling bond states [9, 10]), but are not reported in the EPR measurements. Instead, under hydrogenation an increase of the EPR-resonance at $g=2.0052$ is observed [8, 11]. If this effect is directly related to the adsorbed molecules or simply a consequence of a shift of the Fermi level is still in discussion.

In this work we show that the *ab initio* calculation of g -tensors can help to elucidate the situation in $\mu\text{c-Si:H}$. We calculate the elements of the electronic g -tensor for some paramagnetic states at silicon surfaces from first principles, using a recently developed gauge-including projector augmented plane wave (GI-PAW) approach [1, 12] in the framework of DFT. According to the in-diffusion of water

and atmospheric gases [8] we investigate the EPR fingerprint of those paramagnetic states that are created by hydrogen adsorbed at Si(111) and Si(001) surfaces. Our approach is shown to be able to distinguish between different surface states. For silicon surfaces with different hydrogen coverages, the g -tensor is by far more characteristic than the hf splitting of the Si dangling bonds or that of the adsorbed H atoms.

2 Computational Our first-principles calculations of the EPR parameters are based on density functional theory (DFT) using the gradient-corrected PBE functional in its spin-polarized form [13]. The hyperfine splittings are calculated taking into account relativistic effects in scalar-relativistic approximation [14]. Whereas the hf splittings depend on the magnetization density $m(\mathbf{r}) = n^\uparrow(\mathbf{r}) - n^\downarrow(\mathbf{r})$ exclusively, the main deviation of the g -tensor from its free electron value $g_e \approx 2.002\,319\,278$ is given by the spin-orbit coupling of the many-particle system. In physically transparent form it can be written in terms of spin-polarised electron currents $\mathbf{j}_\uparrow^{(1),\mu}$ and $\mathbf{j}_\downarrow^{(1),\mu}$ induced by a unit magnetic field \mathbf{B}^μ applied along the direction μ :

$$\Delta g_{\mu\nu}^{\text{SO}} = \frac{\alpha}{2S} \left[\sum_{\sigma=\pm 1(\uparrow,\downarrow)} \sigma \int \nabla V_{\text{eff}}^\sigma \times \mathbf{j}_\sigma^{(1),\mu}(\mathbf{r}) d^3r \right]_\nu \quad (1)$$

whereby this result is obtained via perturbation theory from Dirac's equation in the presence of spin-orbit coupling and an external magnetic field. α is the fine structure constant, S the total spin given by the number of unpaired electrons times 1/2. $\nabla V_{\text{eff}}^\sigma$ denotes the gradient of the spin-polarized effective potential. Besides ground state quantities the evaluation of the g -tensor requires the calculation of the spin-currents $\mathbf{j}_\sigma^{(1),\mu}$ in linear magnetic response [12]:

$$\mathbf{j}_\sigma^{(1),\mu}(\mathbf{r}) = 2 \sum_o \text{Re} \left\langle \psi_{(0),o}^\sigma | \mathcal{J}^p \mathcal{G}^\sigma(\epsilon_o) \mathcal{H}_{(1)} | \psi_{(0),o}^\sigma \right\rangle - \frac{\alpha}{2} n^\sigma(\mathbf{r}) \cdot \mathbf{B}^\mu \times \mathbf{r} \quad (2)$$

$\mathcal{J}^p = \frac{1}{2} \frac{\nabla}{i} |\mathbf{r}\rangle \langle \mathbf{r}| + c.c.$ denotes the current operator for vanishing magnetic field. $\mathcal{H}_{(1)} = \frac{\alpha}{2} \mathbf{L} \cdot \mathbf{B}^\mu$ describes the influence of the *uniform* magnetic field onto the system determining the perturbed wavefunctions $|\psi_{(1),o}^\sigma\rangle = \mathcal{G}^\sigma(\epsilon_o) \mathcal{H}_{(1)} |\psi_{(0),o}^\sigma\rangle$ via Green's function of the unperturbed system

$$\mathcal{G}^\sigma(\epsilon) = \sum_e \frac{|\psi_{(0),e}^\sigma\rangle \langle \psi_{(0),e}^\sigma|}{\epsilon - \epsilon_e^\sigma}$$

whereby the sum runs over the *empty* orbitals e .

Strictly seen, the formalism so far presented ensures only a faithful description of the nuclear and two-electron spin-orbital coupling. According Ref. [1] higher order

contributions can be approximately taken into account via the *spin-other-orbit correction*, given by the screening $\mathbf{B}^{(1),\mu}(\mathbf{r})$ of the external magnetic field \mathbf{B}^μ by the induced currents as experienced by the unpaired electrons:

$$\Delta g_{\mu\nu}^{\text{SOO}} = \frac{g_e \alpha}{2S} \int \mathbf{e}_\nu \cdot \mathbf{B}^{(1),\mu}(\mathbf{r}) m(\mathbf{r}) d^3r \quad (3)$$

whereby the screening is given by applying Biot-Savart's law

$$\mathbf{B}^{(1),\mu}(\mathbf{r}) = \alpha \int \mathbf{j}^{(1),\mu} [n(\mathbf{r}) - m(\mathbf{r})] \times \frac{\mathbf{r} - \mathbf{r}'}{|\mathbf{r} - \mathbf{r}'|^3} d^3r$$

The subtracted term $m(\mathbf{r})$ accounts for a 'self-interaction' correction preventing the unpaired electrons from 'feeling' their own magnetic field. In the case of the paramagnetic states at Si surfaces the contribution of the SOO-term comes out to be very small (clearly below 10 ppm). In other words, the spin-other-orbit contributions do not contribute considerably to the g -values given in the Tables 2 – 4.

For a modelling of the surfaces we use supercells and periodic boundary conditions. Hence, the explicit treatment of an external magnetic field \mathbf{B} has to be done in a gauge-invariant way in order to retain the translation invariance of the wavefunctions. Here, the gauge-including projector augmented plane wave (GI-PAW) approach satisfies this requirement and allows an *ab-initio* calculation of the all-electron magnetic response using an efficient pseudopotential approach [1, 12]. Recently, the GI-PAW approach has been implemented in the pwscf-code (QUANTUM-ESPRESSO package) [15] and have been already applied successfully to identify paramagnetic defect structures in SiC and GaN [2–4].

To model the Si(001) surfaces eight layers Si atoms are treated in a 4×4 supercell, whereby the lowest Si layer was saturated with H atoms. To ensure a well defined transition to bulk material, the atoms in the lowest three layers (two Si layers and the H saturation layer) were kept on their ideal bulk positions. All other atoms were allowed to relax freely. To minimize the interaction of the periodic images of the surface, 10 Å vacuum is inserted. We have carefully checked the convergence of the results with respect to the choice of the slab geometry: e.g. by extending the vacuum to 30 Å, we obtain within 1 ppm the same g -values. Using the smaller slab geometry, the *ab initio* calculation of the g -tensor is still rather time-consuming: We use supercells containing up to 175 atoms and norm-conserving pseudopotentials with a plane wave energy cutoff of 30 Ry. Whereas for the geometry optimisation a $2 \times 2 \times 1$ Monkhorst-Pack (MP) [16] k -point set comes out to be sufficient, to obtain reasonably converged estimates for the g -tensor in the general case at least $4 \times 4 \times 1$ samplings come out to be unavoidable (see the Si(001):H in Table 4 as an example). In the case of C_{1h} symmetry e.g. the number of k -points can be reduced by symmetry to 4, but the

Table 1 Largest hf splittings [MHz] of a H vacancy at Si(111):H surface as calculated by *ab initio* DFT. θ denotes the angle between the principal axis of the hf tensor and the surface normal. All hf splittings due to H atoms are below 2 MHz.

| | # nuclei | A_1 | A_2 | A_3 | θ |
|--------|----------|--------|--------|--------|----------|
| Si_1 | 1 | -220.0 | -220.0 | -414.9 | 0.0° |
| Si_2 | 3 | 1.4 | 0.0 | -6.7 | 52.1° |
| Si_3 | 3 | -26.5 | -27.4 | -42.8 | 0.4° |
| Si_4 | 3 | -20.1 | -20.4 | -26.7 | 66.3° |
| Si_5 | 3 | -7.5 | -7.7 | -10.4 | 10.0° |

number of $(k + q)$ -points has to be multiplied by a factor of seven in order to obtain the derivatives in the reciprocal space required to calculate the spin-currents in linear magnetic response [12]. By this requirements the calculation of a g -tensor takes about an order of magnitude more computational time than structure optimization.

3 Results We first discuss the H vacancy at a Si(111):H surface as a reference system. It provides a simple model for a single paramagnetic dangling bond at an otherwise completely hydrogenated surface. Fig. 1 shows several views of the microscopic structure and the corresponding magnetisation density $m(\mathbf{r})$. As can be seen from the top view in the lower left corner, the structure shows perfect C_{3v} symmetry with the symmetry axis along the surface normal. An analysis of $m(\mathbf{r})$ at the nuclei leads to the hyperfine splittings given in Table 1. As intuitively expected, the by far largest hf splitting (-415 MHz and -220 MHz for the magnetic field along and perpendicular to the surface normal, respectively) is due to the unsaturated Si-atom at the surface. Fig. 2 shows the magnetization density in a plane parallel to the surface normal and, by this, a typical 'textbook' fingerprint of a dangling bond. As an additional feature, a weaker accumulation of $m(\mathbf{r})$ is found centered at three equivalent Si-atoms (see also Fig. 1) in the third Si-layer, again roughly aligned along the surface

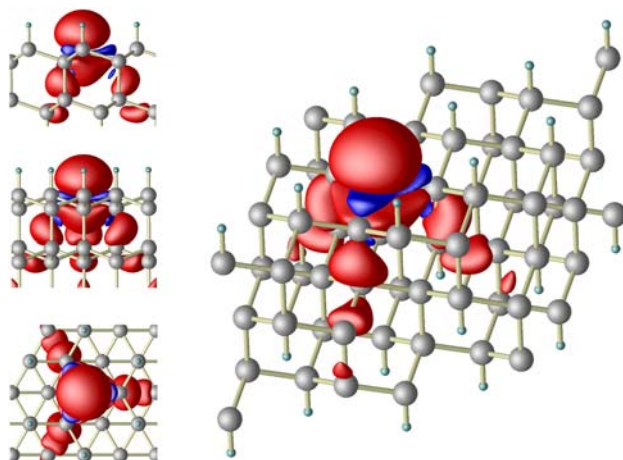


Figure 1 Microscopic structure and magnetisation density of the paramagnetic H vacancy at Si(111):H surface for different side views (lower left corner: top view).

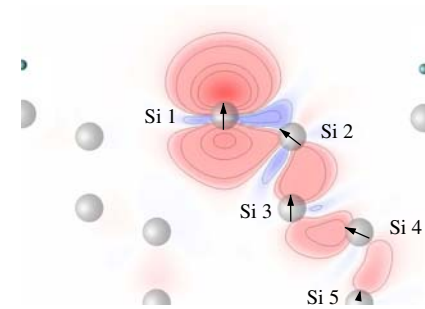


Figure 2 Plot of the magnetisation density for a H vacancy at Si(111):H surface within a plane including the surface normal - a textbook dangling bond (see also text). The arrows describe the direction of the magnetization density at the Si-nuclei.

normal. As a result, besides that of the dangling bond itself, our *ab initio* calculations predicts a further characteristic hf splitting due to these three equivalent Si nuclei. With a value of about -43 MHz the hf splitting could be large enough to be resolved in EPR measurements. In contrast, the hf splittings below 10 MHz (see also Table 1), especially that of the H atoms at the Si(111) surface (below 2 MHz) are too small to be resolved. They will contribute to the width of the central line instead.

The position of the central line is determined by the g -tensor. In Table 2, the calculated principal values are compiled for different k -point samplings. At least for the $3 \times 3 \times 1$ and larger samplings the values can be considered converged. The vanishing angle θ between g_3 and the surface normal and the equivalence of the lateral values g_1 and g_2 are due to the C_{3v} -symmetry confirming again the perfect alignment of the dangling bond along the surface normal. Perpendicular to the surface normal with 2.00939 a comparatively large g -value is predicted. The g -value parallel to the surface normal remains more similar to that of the free electron. The reason for this particular anisotropic shape is the perfect alignment of the dangling bond along the surface normal resulting in a strongly anisotropic spin-orbit coupling similar to the Rashba-type [17] characterized by vanishing spin-orbit coupling for the spin along the surface normal.

The situation becomes more difficult in case of the Si(001) surface that has an appreciable history of both experimental and theoretical work (see e.g. Ref. [18] for a review). It shows the famous 2×1 reconstruction into rows

Table 2 k -point convergence of the g -tensor for the H vacancy at Si(111):H surface ($g_e \approx 2.00232$). θ denotes the angle between the principal axis g_3 and the surface normal.

| k -point mesh | g_1 | g_2 | g_3 | θ |
|-----------------------|---------|---------|---------|----------|
| Γ | 2.01250 | 2.01250 | 2.00766 | 0.0° |
| $2 \times 2 \times 1$ | 2.00925 | 2.00925 | 2.00068 | 0.0° |
| $3 \times 3 \times 1$ | 2.00939 | 2.00939 | 2.00104 | 0.0° |
| $4 \times 4 \times 1$ | 2.00939 | 2.00939 | 2.00111 | 0.0° |
| $5 \times 5 \times 1$ | 2.00939 | 2.00939 | 2.00111 | 0.0° |
| $6 \times 6 \times 1$ | 2.00939 | 2.00939 | 2.00111 | 0.0° |

Table 3 Comparison of the calculated g -tensors for a single adsorbed H-atom and for a nearly complete H-coverage of the Si(001) surface. For a better comparison with the calculated hf splittings [MHz] the calculated Δg -values are given in ppm.

| | A_1 | A_2 | A_3 | θ_{hf} | $\Delta\bar{g}$ | Δg_1 | Δg_2 | Δg_3 | θ |
|-----------------------------------|-------|-------|-------|----------------------|-----------------|--------------|--------------|--------------|----------|
| (111): H saturated with H vacancy | -220 | -220 | -415 | 0° | 4309 | 7070 | 7070 | -1213 | 0.0° |
| (001): single adsorbed H atom | -189 | -189 | -373 | 18° | -2149 | -2079 | -219 | -4139 | 27.8° |
| (001): monohydride with H vacancy | -254 | -255 | -450 | 20° | 2941 | 5841 | 3431 | -449 | 33.5° |

of buckling Si dimers. The left part of Fig. 3 shows a side view along these dimer rows. The adsorption of a single H atom breaks the double bond of a dimer, leading to a single dangling bond (left row but one in Fig. 3). According to our total energy calculations, the H atom is more likely to be adsorbed at the upper Si atom of a tilted dimer. In Table 4 the corresponding g -tensors calculated for different k -point samplings are given. As already mentioned above, to achieve a reasonable estimate for the angle θ (about 28°), a $4 \times 4 \times 1$ MP set comes out to be unavoidable.

If further H atoms are adsorbed at the Si(001) surface, either further dimers are broken or existing dangling bonds are saturated. In the case of complete saturation, each Si atom at the surface bonds one H atom. In Table 3, the EPR parameters for a H vacancy at such a Si(001) monohydride surface (see right part of Fig. 3) are compared with that for a single adsorbed H atom.

Obviously, the g -tensor varies critically with the hydrogen coverage. Especially the Δg_3 -values along the principal axis of the g -tensor differ by more than one order of magnitude. In this sense, the g -tensor is by far more characteristic than the hf splittings of the adsorbed H atoms and the Si dangling bonds that vary only within 20%. Since in contrast to the hf splittings the sign of Δg can be determined experimentally, this holds also in case of powder spectra where only the isotropic part \bar{g} is available from experiment. E.g. an analysis of the H coverage at the surfaces in $\mu\text{C-Si:H}$ could become possible. Hence, the *ab initio* calculation of the g -tensor should be in general a basic key to a better understanding of the microscopic structure of paramagnetic surfaces and interfaces.

Acknowledgements U.G. is grateful to acknowledge financial support by the Deutsche Forschungsgemeinschaft (DFG, Grant No. GE 1260/3-1) and by the Centre National de la Recherche Scientifique (CNRS, France). The time-consuming

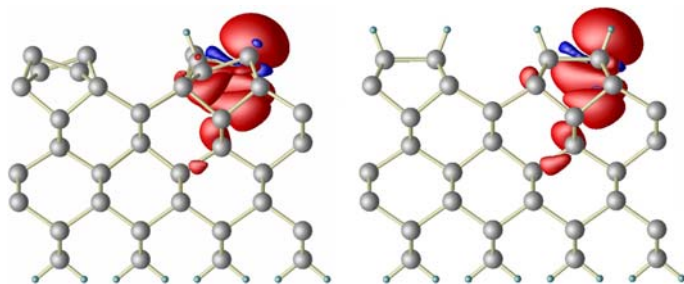


Figure 3 Structure and magnetisation densities for a single adsorbed H-atom (left) and for a nearly complete H-coverage of the Si(001) surface (H vacancy at monohydride surface, right).

calculations were done at the PC² Paderborn and at the HLRS supercomputing center Stuttgart.

References

- [1] Ch.J. Pickard and F. Mauri, Phys. Rev. Lett. **88**, 086403 (2002).
- [2] U. Gerstmann, E. Rauls, S. Greulich-Weber, E.N. Kalabukhova, D.V. Savchenko, A. Pöpl, and F. Mauri, Mater. Sci. Forum **556-557**, 391 (2006).
- [3] U. Gerstmann, A.P. Seitsonen, F. Mauri, and J. von Bardeleben, Mater. Sci. Forum **615-617**, 357 (2009).
- [4] U. Gerstmann, A.P. Seitsonen, and F. Mauri, Phys. Status Solidi B **245**, 924 (2008).
- [5] E. Vallet-Sauvain, U. Kroll, J. Meier, A. Sah, and J. Pohl, J. Appl. Phys. **87**, 3137 (2000).
- [6] D.L. Staebler, C.R. Wronski, Appl. Phys. Lett. **31**, 292 (1977).
- [7] S. Klein, F. Finger, R. Carius, T.Dylla, B. Rech, M. Grimm, L. Houben, and M. Stutzmann, Thin Solid Films **430**, 202, (2003).
- [8] F. Finger, R. Carius, T. Dylla, S. Klein, S. Okur, and M. Günes, IEE Proc.-Circuits Devices Syst. **150**, 309 (2003).
- [9] J.L. Cantin, M. Schoisswohl, and H.J. von Bardeleben, Phys. Rev. B **52**, R11599 (1995).
- [10] B. Langhanki, S. Greulich-Weber, J.-M. Spaeth, and J. Michel, Appl. Phys. Lett. **78**, 3633 (2001).
- [11] J. Behrends et al., J. Non-Cryst. Solids **354**, 2411 (2008).
- [12] Ch.J. Pickard and F. Mauri, Phys. Rev. B **63**, 245101 (2001).
- [13] J. P. Perdew, K. Burke, and M. Ernzerhof, Phys. Rev. Lett. **78**, 1396 (1997).
- [14] P.E. Blöchl, Phys. Rev. B **62**, 6158 (2000).
- [15] P. Giannozzi et al., J. Phys.: Condens. Matter **21**, 395502 (2009); <http://www.quantum-espresso.org>.
- [16] H.J. Monkhorst and J.D. Pack, Phys. Rev. B **13**, 5188 (1976).
- [17] E.I. Rashba, Fiz. Tverd. Tela **2**, 1224 (1960); Sov. Phys. Solid State **2**, 1109 (1960).
- [18] J. Dabrowski, in: Silicon Surfaces and Formation of Interfaces, ed. by J. Dabrowski and H.J. Müssig (World Scientific, Singapore 2000), pp. 82-204.

Table 4 k -point convergence of the g -tensor for an H-atom adsorbed at the Si(001) surface. θ denotes the angle between the principal axis g_3 and the surface normal.

| k -point mesh | g_1 | g_2 | g_3 | θ |
|-----------------------|---------|---------|---------|----------|
| Γ | 1.99643 | 1.99793 | 1.98935 | 79.7° |
| $2 \times 2 \times 1$ | 2.00307 | 2.00190 | 1.99995 | 64.8° |
| $3 \times 3 \times 1$ | 2.00123 | 2.00201 | 1.99915 | 45.4° |
| $4 \times 4 \times 1$ | 2.00021 | 2.00209 | 1.99820 | 27.6° |
| $5 \times 5 \times 1$ | 2.00019 | 2.00209 | 1.99812 | 27.6° |
| $6 \times 6 \times 1$ | 2.00024 | 2.00210 | 1.99818 | 27.8° |